



OPEN

PdNPs/NiNWs as a welding tool for the synthesis of polyfluorene derivatives by Suzuki polycondensation under microwave radiation

Tomasz Wasiak¹, Dominik Just¹, Andrzej Dzieńia¹, Dariusz Łukowiec², Stanisław Wacławek³, Anna Mielańczyk¹, Sonika Kodan⁴, Ananya Bansal⁴, Ramesh Chandra⁴ & Dawid Janas¹✉

Conjugated polymers are promising tools to differentiate various types of semiconducting single-walled carbon nanotubes (s-SWCNTs). However, their synthesis is challenging. Insufficient control over molecular weights, and unpredictable/unrepeatable batches hinder possible applications and scale-up. Furthermore, commercial homogeneous catalysts often require inert conditions and are almost impossible to recycle. To overcome these problems, we present a nanocatalyst consisting of magnetic nickel nanowires decorated with highly active palladium nanoparticles. A two-step wet chemical reduction protocol with the assistance of sonochemistry was employed to obtain a heterogeneous catalyst capable of conducting step-growth Suzuki polycondensation of a fluorene-based monomer. Additionally, we enhanced the performance of our catalytic system via controlled microwave irradiation, which significantly shortened the reaction time from 3 d to only 1 h. We studied the influence of the main process parameters on the yield and polymer chain length to gain insight into phenomena occurring in the presence of metallic species under microwave irradiation. Finally, the produced polymers were used to extract specific s-SWCNTs by conjugated polymer extraction to validate their utility.

Polymers are one of the most diverse and versatile groups of chemical compounds. Recently, π -conjugated polymers have emerged as highly electroactive and photoactive materials, which can be used to craft various electronic devices^{1,2}. Most of their applications involve photovoltaics^{3,4}, memory devices, or organic light-emitting diodes (OLEDs)^{5,6}. However, they are considered almost indispensable in the field of chirality selective sorting of single-walled carbon nanotubes (SWCNTs).

SWCNTs are produced by various methods such as arc discharge (AD)⁷, pulsed laser vaporization (PLV)⁸, and chemical vapor deposition (CVD)⁹, to name a few. Unfortunately, among these approaches, the final product is obtained as a mixture of SWCNTs of different types (both metallic and semiconducting), which greatly reduces their research diversity and implementation potential. Therefore, these raw materials must be subsequently processed to isolate SWCNTs of individual types. Currently, a spectrum of methods is available for SWCNT purification¹⁰. One of the most convenient and effective techniques is conjugated polymer extraction (CPE). Polymers readily deposit on the SWCNT surface due to formed π - π or CH- π interactions. Crucially, depending on the structure of the polymer, these materials exhibit different selectivity toward specific SWCNT types¹¹. Consequently, conjugated polymers may harvest only the desired species from a raw polychiral material. Promising results have been published for poly(9,9-dioctylfluorenyl-2,7-diyl) (PFO) and its derivatives such as poly(9,9-dioctylfluorene-*alt*-1,4-benzo-(2,10,3)-thiadiazole) (F8BT)¹². Among the evaluated polymers, PFO exhibits superior selectivity for processing small-diameter s-SWCNTs in 0.8–1.2 nm range. In particular,

¹Department of Chemistry, Silesian University of Technology, B. Krzywoustego 4, 44-100 Gliwice, Poland. ²Materials Research Laboratory, Faculty of Mechanical Engineering, Silesian University of Technology, Konarskiego 18a, 44-100 Gliwice, Poland. ³Institute for Nanomaterials, Advanced Technologies and Innovation, Technical University of Liberec, Studentská 1402/2, 461 17 Liberec 1, Czech Republic. ⁴Nanoscience Laboratory, Institute Instrumentation Centre, Indian Institute of Technology Roorkee, Roorkee 247667, India. ✉email: Dawid.Janas@gmail.com

it offers exceptional performance, enabling monochiral resolution, suspending only (7,5)^{13,14} or (7,3)¹⁵ SWCNTs under specific conditions.

Despite the advantages related to the CPE approach, the synthesis of conjugated polymers via coupling reactions is difficult to control and optimize. As a result, produced batches commonly have inconsistent molar weights and dispersity indices (*D*). This is a serious issue as it determines the selectivity and yield of the CPE of SWCNTs¹⁶. The most often used methodology to obtain fluorene-based conjugated polymers is the Suzuki polycondensation reaction. It is an A-B or AA-BB type process wherein monomers consisting of diarylbromide moieties and diarylboronate esters are combined. This reaction is commonly catalyzed by Pd complexes such as tetrakis (triphenylphosphine) palladium(0) (Pd(PPh₃)₄), which in most cases provides satisfactory yields. Although it is a highly active and efficient homogeneous catalyst, its high price, arduous synthesis route, air sensitivity, and lack of recyclability hinder scale-up opportunities for the production of conjugated polymers and limit their application scope. However, these obstacles can be overcome via the development of new catalytic systems based on modern materials that can retain high activity and selectivity while simultaneously working in the presence of air for a prolonged time.

Certain nanomaterials fulfill the aforementioned conditions. For instance, reports have shown that palladium nanoparticles (PdNPs) have been successfully implemented for Suzuki cross-coupling reaction of aryl halides containing -methyl, -methoxy, and -nitro moieties^{17–19}, making them excellent candidates for improving the protocol of conjugated polymer synthesis. However, quasi-homogeneous PdNPs are cumbersome to separate from the reaction mixture after polymerization, which reduces their applicability and increases the process costs. Therefore, to overcome this issue, the provision of a heterogeneous character to the catalytic system is a reasonable solution.

In this study, we prepared nickel nanowires (NiNWs) that acted as a scaffold for the deposition of highly active PdNPs. The nanocomposite catalytic system was used for the Suzuki polymerization of fluorene-based moieties. To the best of our knowledge, this is the first reported use of PdNPs/NiNWs nanocomposite in this application. NiNWs were synthesized via simple wet reduction of metal salts²⁰, followed by a sonochemical approach to create PdNPs on their surface²¹. The as-prepared nanocatalyst was employed in conjunction with microwave heating for the synthesis of conjugated polymers based on polyfluorene. The developed method permitted the polymerization process to be significantly accelerated compared to the classical thermal approach^{22–25}. The reaction time was considerably shortened from 3 d to only 1 h, which drastically improved the economics of polymer production. The obtained conjugated polymers were then evaluated as selective SWCNT dispersants for sorting polychiral raw material.

Experimental

A list of reagents and procedures (including synthesis of PdNPs/NiNWs and selective isolation of SWCNTs) and methods for characterization of the materials involved in this study are presented in the SI.

Results and discussion

Catalyst characterization

The support nanomaterials (NiNW) with anisotropic structure were synthesized by simple wet chemical reduction. A magnetic field forced the alignment of paramagnetic Ni²⁺ complexes, which enhanced the step-growth of protonanowire²⁶, resulting in relatively long NiNWs (Fig. 1a). The nanomaterials possessed characteristic spikes along an anisotropic nanostructure, which provided a developed surface area (Fig. 1b). Subsequently, a sonochemical approach was engaged for PdNPs deposition. PdNPs were successfully deposited on NiNW support, and their diameters were in the order of the range of single nanometers according to TEM measurements (Fig. 1c). Additionally, ICP-OES was used to determine that Pd concentration was 0.34%, which was employed for calculating TOF values in further catalytic tests.

XRD patterns confirmed the presence of Ni and Pd atoms in the material (Fig. 2a). Three features related to Ni at $2\theta = 44.6^\circ$, 52° , and 76.6° were indexed as (111), (200), and (220) lattice planes, respectively (JCPDS card, File No. 04-0850). They were detected in pure NiNWs before Pd deposition, supporting this assignment (Fig. S4). The peaks at 40.3° (111), 46.8° (200), 68.3° (220), and 82.1° (311) were related to Pd (JCPDS card, File No. 46-1043), which indicated the presence of a face-centered cubic phase. Selected Area Electron Diffraction

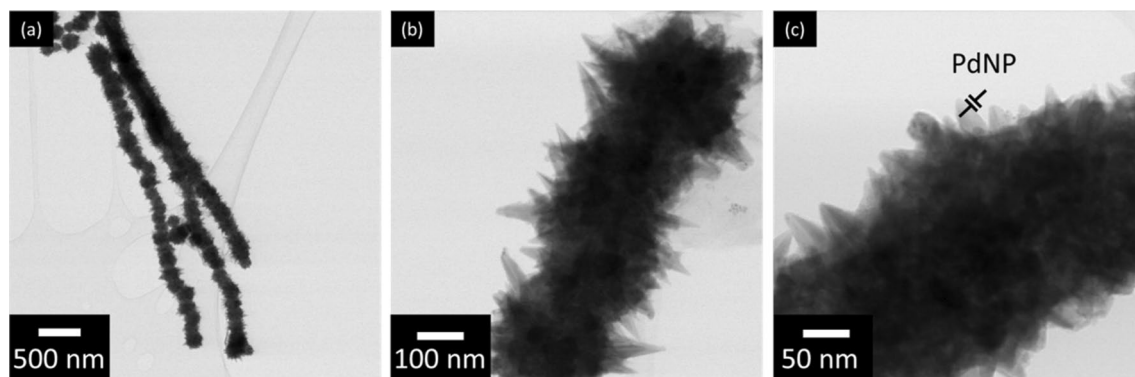


Figure 1. TEM micrographs of PdNPs/NiNWs nanocatalyst at various magnifications.

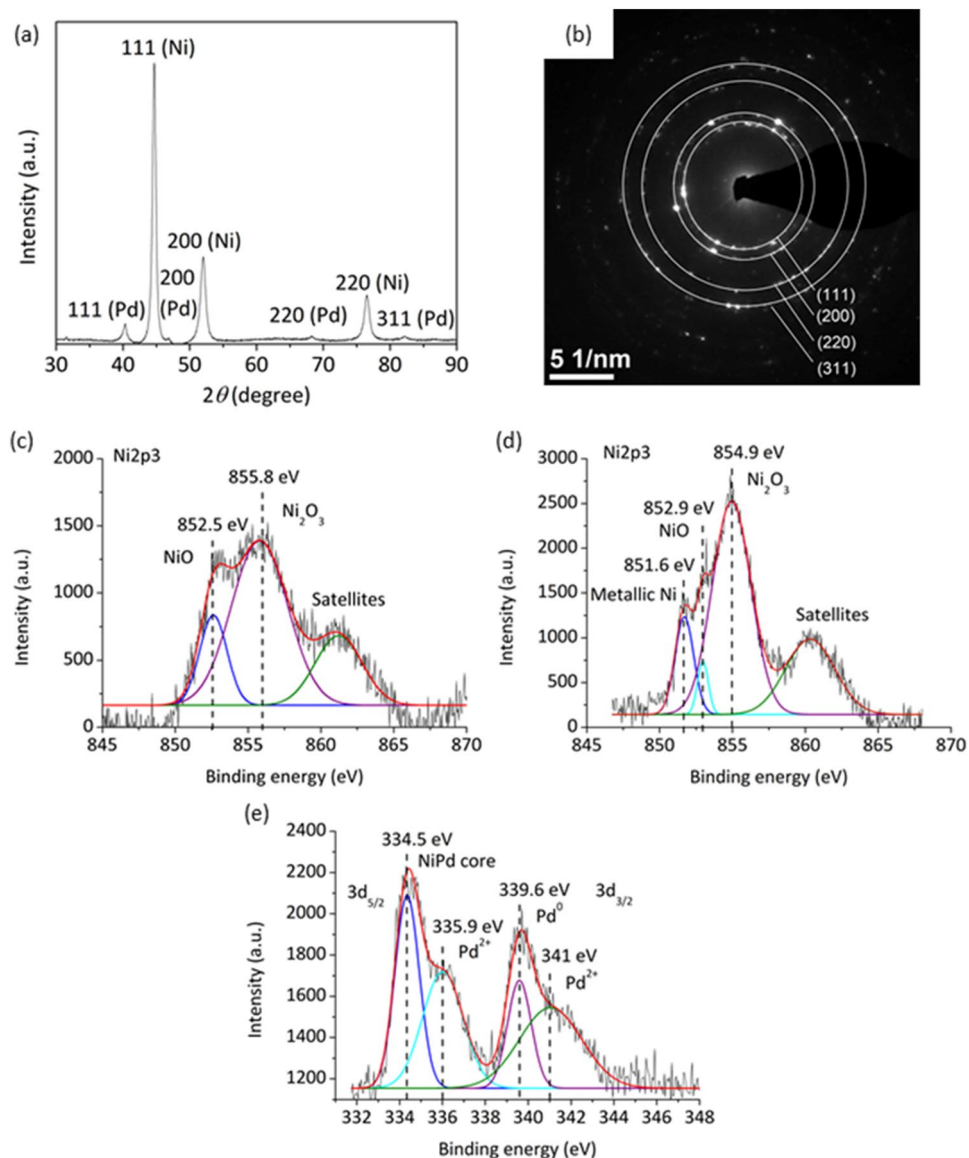


Figure 2. (a) XRD patterns of PdNPs/NiNWs nanocatalyst, (b) SAED patterns of PdNPs/NiNWs nanocatalyst (c) Ni_{2p_{3/2}} of NiNWs, (d) Ni_{2p_{3/2}} of Pd/NiNWs (e) Pd_{3d_{3/2}} and Pd_{3d_{5/2}} X-ray photoemission spectra recorded for PdNPs/NiNWs sample.

(SAED) revealed only Ni patterns (111), (200), (220) and (311). The latter was absent in XRD spectra as its location extended beyond the selected examination range. It should appear at ca. 93.0°. The lack of any Pd-related patterns can be explained by a very small concentration of Pd in the sample (less than 0.5%).

XPS analysis provided relevant information about the electronic states of the catalyst surface. At first, bare NiNWs were analyzed. The obtained spectra showed peaks of NiO and Ni₂O₃ at 852.5 eV and 855.8 eV, respectively, in Ni_{2p_{3/2}} binding energy band. After Pd deposition, a metallic Ni signal was found at 851.6 eV, and nickel oxide signals increased significantly at 852.9 eV (NiO) and 854.9 eV (Ni₂O₃). This can be explained as a result of partial reduction of nickel during sonochemical process and subsequent oxidation in air. Pd showed the binding energies of Pd_{3d_{3/2}} and Pd_{3d_{5/2}}. According to the reference values (340.36 eV and 335.1 eV)²⁷, PdNPs consisted of Pd(0) (339.6 eV) and Pd²⁺ (335.9 eV, 341 eV). Interestingly, the peak at 334.5 eV could represent Pd atoms included in the NiNW core.

Conventional heating route

The study of the catalytic properties involved the standardized procedure for Suzuki polymerization of fluorene-based polymers²⁸. In brief, both monomers were dissolved in toluene, and then an aqueous solution of sodium carbonate was added. As the reaction mixture consisted of two immiscible liquids, the synthesis occurred in an interfacial region. A few drops of Aliquat 336 were added as a phase-transfer catalyst to enhance the mass transport process. Commercially available Pd(PPh₃)₄ catalyst required inert atmospheric conditions, which was

achieved by purging the solution with nitrogen before and after the addition of the catalyst. For PdNPs/NiNWs catalyst, this was unnecessary due to its superior stability in the air. In both tests, the solutions were stirred in closed glass reactors at elevated temperatures. The sealed environment allowed for over-pressure generation and condensation of vapors on the glass walls. After 3 d of vigorous stirring to ensure good contact between both liquid phases, the toluene phase containing Pd(PPh₃)₄ turned black, suggesting the completion of the reaction. In the case of the PdNPs/NiNWs-driven reaction, the top phase turned a yellow color. Polymerization using a commercial catalyst gave a higher yield (83%) compared to the poor initial performance of PdNPs/NiNWs under conventional heating (16%) on the same time scale. Unfortunately, PdNPs/NiNWs nanocatalysts, under the applied conditions, were only able to form oligomers. The elution volume peaks registered for the samples by GPC were only slightly lower than the solvent peak, suggesting that the product comprised mostly of PFO dimers (M_n = 0.909 kg/mol and Đ = 1.24). In contrast, the commercial catalyst-driven reaction gave the expected polymer, characterized by M_n = 15.61 kg/mol and Đ = 3.19. Therefore, while the thermal stimulus was insufficient to activate the PdNPs/NiNWs nanocatalyst, the homogeneous commercial formulation based on Pd(PPh₃)₄ was successful.

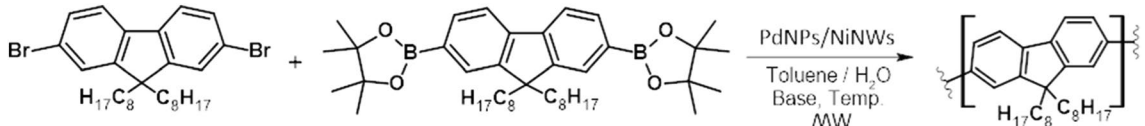
Microwave-assisted route

The various desirable effects of microwave radiation resulting from both thermal and non-thermal effects have been consistently reported in organic synthesis²⁹, but also directly in the area of Suzuki polycondensation³⁰. The irradiation enhances molecular mobility, enabling efficient mixing without the employment of magnetic stirring. This aspect is particularly important owing to the limited performance of PdNPs/NiNWs stemming from the paramagnetic properties of NiNWs. This promotes their accumulation on the surface of the dipole used for stirring the liquid medium in the reactor, possibly reducing the available catalytic surface area. Since, after the first tests, we noticed that the performance achieved by the PdNPs/NiNWs was higher than in analogous reactions supported by conventional heating, hence, we proceeded to optimize the process.

In this study, we focused on Standard (S) and Solid Phase Synthesis (SPS) modes of the employed microwave system using a broad range of experimental conditions. The first one used variable power to obtain the target temperature and maintained it at approx. ± 1 °C. In contrast, during SPS mode, the power was constant, which led to a higher temperature hysteresis (ΔT ≈ 5 °C). While the standard protocol provided a comparable intensity of microwave radiation during the process, SPS mode delivered the power in pulses. Experiments conducted under standard and SPS conditions are listed below (Table 1).

The experiments shown in the table showed a significant acceleration of the reaction supported by microwave radiation compared to the reaction catalyzed by Pd(PPh₃)₄ in conventional heating. In the latter case, no isolated polymer was formed after 1 h. In addition, for most of the conditions tested, the conversion rate was very high, reaching up to 88% under optimal conditions (typically exceeding 60%). Considering the reduction of these values by losses arriving from product isolation, the performance seemed promising.

The observed reaction acceleration was highly beneficial and may lead to the development of more approachable polymer production. A shorter reaction time (1 h compared to 3 d for conventional heating) can reduce



No	Mode	Power [W]	Base/Conc	Temp. [°C]	Yield [%]	TOF [h ⁻¹]	M _n [kg/mol]	M _w [kg/mol]	Đ	Degree of polymerization
1	S	0–200	Na ₂ CO ₃ /1 M	80	0	–	–	–	–	–
2	S	0–200	Na ₂ CO ₃ /1 M	110	62	1793	1.88	3.06	1.63	5
3	S	0–200	Na ₂ CO ₃ /1 M	130	57	1648	8.08	11.31	1.40	21
4	S	0–200	K ₂ CO ₃ /1 M	80	34	983	3.14	3.99	1.27	8
5	S	0–200	K ₂ CO ₃ /1 M	110	69	1995	5.25	8.45	1.61	14
6	S	0–200	K ₂ CO ₃ /1 M	130	75	2168	4.56	6.61	1.45	12
7	SPS	80	Na ₂ CO ₃ /1 M	75–80	0	–	–	–	–	–
8	SPS	80	Na ₂ CO ₃ /1 M	105–110	82	2371	8.32	16.31	1.96	21
9	SPS	80	Na ₂ CO ₃ /1 M	125–130	41	1185	4.95	6.68	1.35	13
10	SPS	80	K ₂ CO ₃ /1 M	75–80	51	1475	3.45	4.59	1.33	9
11	SPS	80	K ₂ CO ₃ /1 M	105–110	69	1995	6.61	11.90	1.80	17
12	SPS	80	K ₂ CO ₃ /1 M	125–130	60	1735	6.19	8.66	1.40	16
13	SPS	100	Na ₂ CO ₃ /1 M	105–110	88	2544	14.32	25.99	1.82	37
14	SPS	120	Na ₂ CO ₃ /1 M	105–110	78	2255	8.37	12.67	1.51	22

Table 1. Microwave-assisted PFO synthesis via Suzuki polycondensation at standard and SPS mode. Reaction conditions: 0.12 mmol of diarylbromide, 0.12 mmol of diarylboronate ester, 2 mL of base solution, 2 mL of toluene, 1 drop of Aliquat 336, and 10 mg of PdNPs/NiNWs catalyst. The reaction was carried out for 1 h. The degree of polymerization was estimated by dividing M_n by monomer mass (0.388 kg/mol).

process costs considerably, especially in the long term, due to energy saving. Moreover, we demonstrated that the molecular weight (M_w) could be controlled through optimized polymerization using the described approach (M_w in the range of 3–26 kg/mol), which has been rarely reported for thermally-promoted Suzuki polycondensation reactions using typical homogeneous catalysts. Our investigations started with examining the temperature as one of the main parameters during the polymerization process, as it controlled reaction speed. When sodium salt was used, 80 °C was insufficient for the reaction to occur during both modes (Table 1—entries 1 and 7). No signs of the product were discerned. On the other hand, when the temperature of the process was increased to 110 °C, the conditions allowed for the precipitation of the crude product in methanol, which confirmed the presence of oligomers (Table 1—entry 2).

During the Suzuki polycondensation reaction, the choice of base was essential due to its vital role in the palladium catalytic cycle. Both strong and weak bases are typically utilized in the synthetic process depending on substrate structure and reactivity. Strong bases, such as sodium hydroxide (NaOH) or potassium hydroxide (KOH), are used for the deprotonation of the boronic acid monomer, which is crucial for initiating the coupling reaction^{31–33}. Carbonate and phosphate salts are more popular for a wide range of substrates, which are free of steric hindrance. These bases facilitate the formation of quaternized organoboron active species with increased nucleophilicity that react with the Pd catalyst, enabling transmetalation and, thus, the polymerization process³⁴. However, weak bases, such as triethylamine (TEA) or pyridine, can neutralize the acid byproduct produced during the reaction. These weak bases prevent side reactions and help maintain the appropriate pH level of the reaction mixture, ensuring the success of the polymerization. Although their performance is less efficient, they allow for the polymerization of some electron-deficient aryl halides at higher temperatures³⁵. Consequently, the choice of base can have a significant impact on the M_w of PFO during polymerization as it, among other factors, affects the kinetics of the polymerization process. Strong bases promote faster polymerization, leading to polymers with higher M_w ^{36–38}. Conversely, weak bases slow down the reaction rate, resulting in polymers of lower molecular weights^{34,39}.

In the case of the reaction conducted in standard mode, switching to potassium carbonate was beneficial for the experiments conducted at 80 °C and 110 °C due to a substantial increase in M_w values (3.99 and 8.45 kg/mol, respectively, vs. lack of product at 80 °C and 3.06 kg/mol registered for the polymer generated at 110 °C) (Table 1—entries 4 and 5 vs. 1 and 2). Interestingly, a further increase of temperature in this mode to 130 °C was favorable for the reaction using Na_2CO_3 , as M_w was even higher (at the slight expense of the yield) (Table 1—entry 3), the analogous process conducted using K_2CO_3 resulted in reduced M_w with concurrent yield improvement (Table 1—entry 6).

In SPS mode, both cases (sodium and potassium salts) showed a decrease in PFO molecular weights at high process temperatures, especially for sodium carbonate. Additionally, examination of an increase in power while maintaining the same temperature range of 105–110 °C, found that the best results were obtained for 100 W settings (M_w of 25.99 kg/mol, Table 1—entry 13). A lower power of 80 W was insufficient to elongate the polymers to the appreciable extent (M_w of 11.9 kg/mol, Table 1—entry 11). In comparison, a higher power of 120 W did not provide sustainable conditions for the polymer chain growth (M_w of 12.67 kg/mol, Table 1—entry 14). However, in this case, the dispersity decreased from 1.8 to 1.51, which resulted in a slightly higher degree of polymerization (22 vs. 17).

Regarding the impact of the microwave settings on the characteristics of the synthesized polymers, SPS mode provided pulses of constant power in short bursts. This possibly led to the generation of hot spots on the metallic nanostructures upon absorption of radiation^{40–42}, which improved the diffusion of reactants and provided more energy to overcome the thermodynamic barriers of the process. The obtained results confirmed this reasoning due to longer chain polymers being generated using this mode (Table 1—entries 8 and 11). On the contrary, in standard mode, the microwave power was tuned to reach the desired temperature. Hence, the power ranged between 5 and 15 W to maintain the temperature, and over most of the reaction time the reactor provided only a small portion of radiation, which in turn minimized the hot spot effect. Consequently, the diffusion of reactants to reach the catalytic sites (in the absence of mixing) was hindered. This was detrimental to the reaction rate, which lowered the final molar mass of the polymer, especially in the case of entry 2 in Table 1. As mentioned earlier, microwaves accelerate the process in many ways. The lack of temperature gradient in the reaction vessel and faster heating provided more suitable conditions for the reaction. We believed that Pd hot spots acted as welding spots for joining monomers together, which promoted dimerization and further step-growth polymerization (Fig. 3). Therefore, microwaves accelerated the formation of the studied polymers. Finally, regardless of the microwave heating mode, the synthesized PFO polymers were rather homogeneous as \mathcal{D} , describing the heterogeneity of polymer mass, ranging between 1.27 and 1.96 (the lower values corresponded to better control over polymer chain growth during the synthesis). A step-growth polymerization is often characterized by $\mathcal{D} = 2$ ⁴³, so the newly designed approach matched the expectations while substantially shortening the reaction times.

SWCNTs polymer wrapping

One of the intriguing properties of PFO is its high affinity (7,5)-chirality SWCNTs in organic solvents and, thus, its ability to selectively isolate this SWCNT type^{12,14,16,44,45}. When PFO is dissolved in an organic solvent, preferably in nonpolar toluene, it forms a complex with (7,5) SWCNT through π - π stacking interactions⁴⁶. The unique arrangement of atoms in (7,5) SWCNT structure facilitates strong and specific binding with PFO⁴⁷. Consequently, this polymer enables selective isolation of (7,5) SWCNTs from polychiral mixtures. Despite the remarkable selectivity of PFO towards (7,5) SWCNT, challenges remain. The interaction between PFO and SWCNT is influenced by various parameters, such as polymer characteristics and selection of solvent¹⁴ and extraction conditions⁴⁸. Understanding the role of these parameters is crucial for optimizing the selective isolation process.

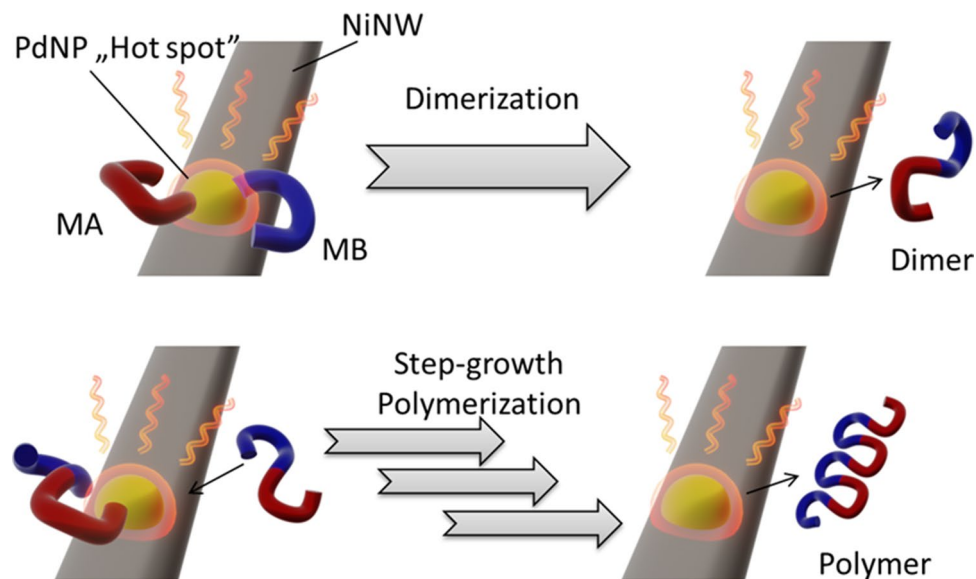


Figure 3. Proposed mechanism of "hot spot" mediated step-growth Suzuki polymerization. MA and MB stand for Monomer A (diaryl bromide) and Monomer B (diaryl boronate ester), respectively.

To address the above-mentioned challenges, first, we analyzed the composition of the raw SWCNT mixture by suspending it non-selectively using poly (9,9-dioctylfluorenyl-2,7-diyl-alt-3-dodecylthiophene-2,5-diyl) (PFO-3DDT) conjugated polymer in toluene. The obtained dispersion was studied using optical absorption spectroscopy and photoluminescence (PL) excitation-emission mapping (Fig. 4a,b). The exact positions of the characteristic bands from S_{11} transitions of specific SWCNTs were previously reported in the literature¹⁵. The dominant chirality in the starting material was (6,5). The amount of (7,5) SWCNTs was also sufficiently high to justify its isolation. This is important because, to date, there is no commercially available raw soot enriched in this particular chirality. In this research, after synthesizing a broad range of PFO polymers, we focused on investigating the influence of M_w of PFO on its preference for (7,5) SWCNT wrapping. To this end, the polymers were tested using the model CPE process described in detail in SI. By varying M_w of PFO, we found that it played a significant role in the selectivity of the isolation process. The shape of the peaks (their full width at half maxima) and the peak-to-valley ratios^{49–52} determined the quality of SWCNT wrapping. In the case of low-molecular-weight polymers, the spectra were not sufficiently sharp, excluding the possibility of confirming the identity of peaks arising from specific chiralities. Hence, the polymer could not properly individualize SWCNTs, therefore, SWCNT bundles were present in the suspension instead. Furthermore, polymers with an average M_w above 8 kg/mol exhibited stronger interactions with (7,5) SWCNTs (Fig. 4c), resulting in enhanced selectivity for this SWCNT type. This was manifested by the appearance of S_{11} transition at 1040 nm. Concomitantly, the sharper shape of the peaks, indicative of SWCNT debundling, confirmed that their individualization was crucial to unlocking the possibility of material purification. A further increase of the polymer M_w , steadily increased the ratio of (7,5) SWCNT peak to that of different species. At M_w of approx. 16 kg/mol, a critical polymer chain length was reached to promote satisfactory separation results since only (7,5) SWCNTs were suspended. The process of CPE involves dynamic adsorption and desorption of polymer chains on/from the SWCNT surface. To achieve successful isolation, a polymer must interact favorably only with a single SWCNT type sufficiently to remain on its surface during sonication and subsequent centrifugation. In our case, we determined that once the polymer reached this threshold M_w , its adsorption rate on (7,5) SWCNTs significantly exceeded the tendency to desorb (or the desorption energy was higher than that provided by sonication). Either way, the PFO chains gradually accumulated on the (7,5) SWCNT surface reducing the amount of available for other chiralities. As a result, other SWCNTs wrapped to a smaller extent were very unstable in solution and susceptible to reaggregation during centrifugation. Hence, the amount of various chiralities in dispersion decreased rapidly. As shown in the excitation-emission PL map of suspension obtained by sonicating in-house made PFO and raw SWCNTs in toluene, the SWCNT dispersion had a monochiral character (Fig. 4d).

Conclusions and future perspectives

We successfully developed a PdNPs/NiNWs nanocomposite catalytic system, which was highly active in polymerization by Suzuki coupling. We obtained PFOs with quantitative efficiency with a wide range of M_w , which helped gain insight into nanoscale phenomena such as the CPE process. A microwave-assisted synthesis reduced the reaction time from 3 d to 1 h, thereby markedly improving the economics of the process. The microwave heating also provided optimum distribution of energy to reaction volume, because of which the characteristics of the products were more favorable. Dispersity indices of less than 2 were achieved for all obtained polymers. Optimization of power, base, temperature, and time resulted in the production of high-quality polymers, which were employed in SWCNT purification. Our findings revealed a direct correlation between the length of polymer

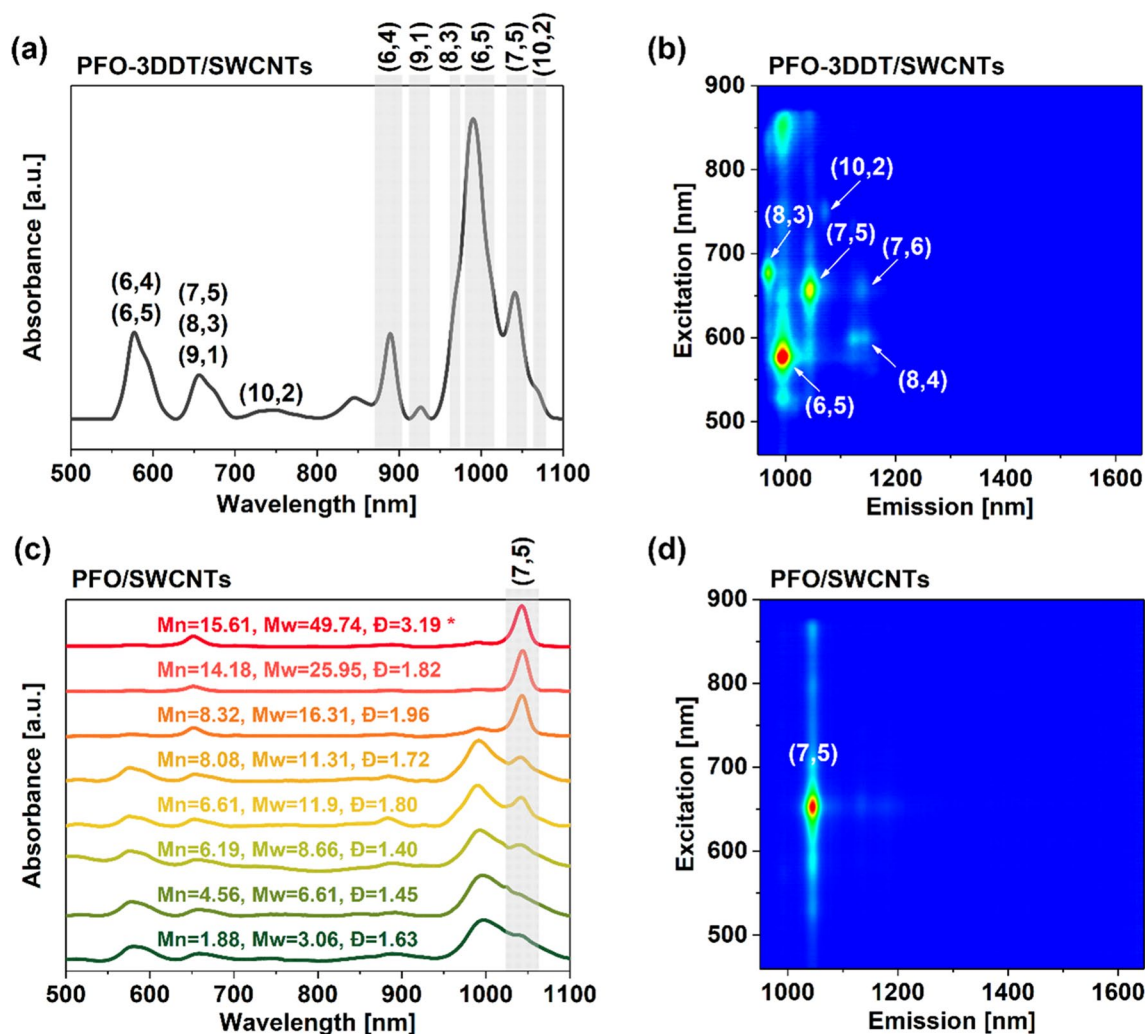


Figure 4. (a) UV–VIS spectrum of SWCNTs suspended by PFO-3DDT. (b) Excitation–emission PL map of SWCNTs suspended by PFO-3DDT ((6,4) and (9,1) SWCNTs are not visible as they emit outside of the measurement range). (c) The influence of molecular characteristics of the synthesized PFO batches on the optical absorbance spectra of SWCNTs suspended with PFO. *The polymer with the highest M_w (49.74 kg/mol) refers to Pd(PPh₃)₄-driven reaction, which is shown here as a reference. All the other polymers were obtained using PdNPs/NiNWs nanocatalyst. (d) Excitation–emission PL map of extracted (7,5) SWCNTs using PFO synthesized using the specified conditions (Table 1, entry 13).

chains and the selectivity towards desired chirality, with longer chains demonstrating higher selectivity. Intriguingly, we identified a specific M_w threshold, notably at 16.30 kg/mol, corresponding to 20 dimers units for PFO, which gave rise to significant improvement of SWCNT selectivity. Overall, the obtained results pave the way for the design of polymers with considerable application opportunities in materials science, with already documented high utility for purifying SWCNTs.

Data availability

The raw/processed data required to reproduce these findings cannot be shared at this time as the data also forms part of an ongoing study.

Received: 22 November 2023; Accepted: 23 January 2024

Published online: 28 January 2024

References

- Guo, X., Baumgarten, M. & Müllen, K. Designing π -conjugated polymers for organic electronics. *Prog. Polym. Sci.* **38**, 1832–1908. <https://doi.org/10.1016/J.PROGPOLYMSCI.2013.09.005> (2013).
- Moliton, A. & Hiorns, R. C. Review of electronic and optical properties of semiconducting π -conjugated polymers: Applications in optoelectronics. *Polym. Int.* **53**, 1397–1412. <https://doi.org/10.1002/PLI.1587> (2004).
- Cheng, Y. J., Yang, S. H. & Hsu, C. S. Synthesis of conjugated polymers for organic solar cell applications. *Chem. Rev.* **109**, 5868–5923. https://doi.org/10.1021/CR900182S/ASSET/IMAGES/LARGE/CR-2009-00182S_0062.JPEG (2009).
- Wöhrle, D. & Meissner, D. Organic solar cells. *Adv. Mater.* **3**, 129–138. <https://doi.org/10.1002/adma.19910030303> (1991).

5. Grimsdale, A. C., Leok Chan, K., Martin, R. E., Jokisz, P. G. & Holmes, A. B. Synthesis of light-emitting conjugated polymers for applications in electroluminescent devices. *Chem. Rev.* **109**, 897–1091. <https://doi.org/10.1021/cr000013v> (2009).
6. Burroughes, J. H. *et al.* Light-emitting diodes based on conjugated polymers. *Nature* **347**, 539–541. <https://doi.org/10.1038/347539a0> (1990).
7. Iijima, S. & Ichihashi, T. Single-shell carbon nanotubes of 1-nm diameter. *Nature* **363**, 603–605. <https://doi.org/10.1038/363603a0> (1993).
8. Guo, T., Nikolaev, P., Thess, A., Colbert, D. T. & Smalley, R. E. Catalytic growth of single-walled nanotubes by laser vaporization. *Chem. Phys. Lett.* **243**, 49–54. [https://doi.org/10.1016/0009-2614\(95\)00825-O](https://doi.org/10.1016/0009-2614(95)00825-O) (1995).
9. José-Yacamán, M., Miki-Yoshida, M., Rendón, L. & Santiesteban, J. G. Catalytic growth of carbon microtubules with fullerene structure. *Appl. Phys. Lett.* **62**, 657–659. <https://doi.org/10.1063/1.108857> (1993).
10. Janas, D. Towards monochiral carbon nanotubes: A review of progress in the sorting of single-walled carbon nanotubes. *Mater. Chem. Front.* **2**, 36–63. <https://doi.org/10.1039/C7QM00427C> (2018).
11. Fong, D. & Adronov, A. Recent developments in the selective dispersion of single-walled carbon nanotubes using conjugated polymers. *Chem. Sci.* **8**, 7292–7305. <https://doi.org/10.1039/C7SC02942J> (2017).
12. Nish, A., Hwang, J.-Y., Doig, J. & Nicholas, R. J. Highly selective dispersion of single-walled carbon nanotubes using aromatic polymers. *Nat. Nanotechnol.* **2**, 640–646. <https://doi.org/10.1038/nnano.2007.290> (2007).
13. Sudakov, I. *et al.* Chirality dependence of triplet excitons in (6,5) and (7,5) single-wall carbon nanotubes revealed by optically detected magnetic resonance. *ACS Nano* **17**, 2190–2204. <https://doi.org/10.1021/acsnano.2c08392> (2023).
14. Dzienia, A., Just, D. & Janas, D. Solvatochromism in SWCNTs suspended by conjugated polymers in organic solvents. *Nanoscale* **15**, 9510–9524. <https://doi.org/10.1039/D3NR00392B> (2023).
15. Dzienia, A. *et al.* Mixed-solvent engineering as a way around the trade-off between yield and purity of (7,3) single-walled carbon nanotubes obtained using conjugated polymer extraction. *Small* <https://doi.org/10.1002/sml.202304211> (2023).
16. Ouyang, J. *et al.* Impact of conjugated polymer characteristics on the enrichment of single-chirality single-walled carbon nanotubes. *ACS Appl. Polym. Mater.* **4**, 6239–6254. <https://doi.org/10.1021/acscpm.2c01022> (2022).
17. Wang, J., Xu, B., Sun, H. & Song, G. Palladium nanoparticles supported on functional ionic liquid modified magnetic nanoparticles as recyclable catalyst for room temperature Suzuki reaction. *Tetrahedron Lett.* **54**, 238–241. <https://doi.org/10.1016/j.tetlet.2012.11.009> (2013).
18. Lou, Z., Gu, Q., Liao, Y., Yu, S. & Xue, C. Promoting Pd-catalyzed Suzuki coupling reactions through near-infrared plasmon excitation of WO₃-x nanowires. *Appl. Catal. B Environ.* **184**, 258–263. <https://doi.org/10.1016/j.apcatb.2015.11.037> (2016).
19. Pérez-Lorenzo, M. Palladium nanoparticles as efficient catalysts for Suzuki cross-coupling reactions. *J. Phys. Chem. Lett.* **3**, 167–174. <https://doi.org/10.1021/jz2013984> (2012).
20. Wasiak, T., Przepis, L., Walczak, K. & Janas, D. Nickel nanowires: Synthesis, characterization and application as effective catalysts for the reduction of nitroarenes. *Catalysts* **8**, 566. <https://doi.org/10.3390/catal8110566> (2018).
21. Fujimoto, T., Terauchi, S.-Y., Umehara, H., Kojima, I. & Henderson, W. Sonochemical preparation of single-dispersion metal nanoparticles from metal salts. *Chem. Mater.* **13**, 1057–1060. <https://doi.org/10.1021/cm000910f> (2001).
22. Vázquez-Guilló, R. *et al.* Advantageous microwave-assisted Suzuki polycondensation for the synthesis of aniline-fluorene alternate copolymers as molecular model with solvent sensing properties. *Polymers* **10**, 215. <https://doi.org/10.3390/polym10020215> (2018).
23. Galbrecht, F., Bünnagel, T. W., Scherf, U. & Farrell, T. Microwave-assisted preparation of semiconducting polymers. *Macromol. Rapid Commun.* **28**, 387–394. <https://doi.org/10.1002/marc.200600778> (2007).
24. Nehls, B. S., Földner, S., Preis, E., Farrell, T. & Scherf, U. Microwave-assisted synthesis of 1,5- and 2,6-linked naphthylene-based ladder polymers. *Macromolecules* **38**, 687–694. <https://doi.org/10.1021/ma048595w> (2005).
25. Tsami, A., Yang, X., Farrell, T., Neher, D. & Holder, E. Alternating fluorene-di(thiophene)quinoxaline copolymers via microwave-supported Suzuki cross-coupling reactions. *J. Polym. Sci. Part Polym. Chem.* **46**, 7794–7808. <https://doi.org/10.1002/pola.23081> (2008).
26. Sun, L., Chen, Q., Tang, Y. & Xiong, Y. Formation of one-dimensional nickel wires by chemical reduction of nickel ions under magnetic fields. *Chem. Commun.* <https://doi.org/10.1039/b704689h> (2007).
27. Wagner, B. E. M. C. D., Riggs, W. M., Davis, L. E. & Moulder, J. F. Handbook of X-ray photoelectron spectroscopy, physical electronic divisions. *Minnesota (USA)* <https://doi.org/10.1002/sia.740030412> (1979).
28. E.P.W. M.Inbasekaran, W. Wu, US5777070A, US5777070A, 1998.
29. de la Hoz, A., Diaz-Ortiz, A. & Moreno, A. Microwaves in organic synthesis. Thermal and non-thermal microwave effects. *Chem. Soc. Rev.* **34**, 164–178. <https://doi.org/10.1039/B411438H> (2005).
30. Metzler, L. *et al.* High molecular weight mechanochromic spirodiary main chain copolymers via reproducible microwave-assisted Suzuki polycondensation. *Polym. Chem.* **6**, 3694–3707. <https://doi.org/10.1039/C5PY00141B> (2015).
31. Miyaura, N. & Suzuki, A. Palladium-catalyzed cross-coupling reactions of organoboron compounds. *Chem. Rev.* **95**, 2457–2483. <https://doi.org/10.1021/cr00039a007> (1995).
32. Hassan, J., Sévignon, M., Gozzi, C., Schulz, E. & Lemaire, M. Aryl–Aryl bond formation one century after the discovery of the Ullmann reaction. *Chem. Rev.* **102**, 1359–1470. <https://doi.org/10.1021/cr000664r> (2002).
33. Zou, G. & Falck, J. R. Suzuki–Miyaura cross-coupling of lithium n-alkylborates. *Tetrahedron Lett.* **42**, 5817–5819. [https://doi.org/10.1016/S0040-4039\(01\)01128-5](https://doi.org/10.1016/S0040-4039(01)01128-5) (2001).
34. Krishna, A., Lunchev, A. V. & Grimsdale, A. C. Suzuki polycondensation. In *Synthetic Methods for Conjugated Polymers and Carbon Materials* (eds Leclerc, M. & Morin, J.-F.) 59–95 (Wiley, 2017). <https://doi.org/10.1002/9783527695959.ch2>.
35. Faul, M. M., Ratz, A. M., Sullivan, K. A., Trankle, W. G. & Winneroski, L. L. Synthesis of novel retinoid X receptor-selective retinoids. *J. Org. Chem.* **66**, 5772–5782. <https://doi.org/10.1021/jo0103064> (2001).
36. Zhang, H., Kwong, F. Y., Tian, Y. & Chan, K. S. Base and cation effects on the Suzuki cross-coupling of bulky arylboronic acid with halopyridines: Synthesis of pyridylphenols. *J. Org. Chem.* **63**, 6886–6890. <https://doi.org/10.1021/jo980646y> (1998).
37. Howell, M. T. *et al.* Suzuki–Miyaura catalyst-transfer polymerization: New mechanistic insights. *Polym. Chem.* **14**, 4319–4337. <https://doi.org/10.1039/D3PY00580A> (2023).
38. Gonzalez, J. A. *et al.* MIDA boronates are hydrolysed fast and slow by two different mechanisms. *Nat. Chem.* **8**, 1067–1075. <https://doi.org/10.1038/nchem.2571> (2016).
39. Walczak, R. M., Brookins, R. N., Savage, A. M., van der Aa, E. M. & Reynolds, J. R. Convenient synthesis of functional polyfluorenes via a modified one-pot Suzuki–Miyaura condensation reaction. *Macromolecules* **42**, 1445–1447. <https://doi.org/10.1021/ma802462v> (2009).
40. Horikoshi, S., Osawa, A., Abe, M. & Serpone, N. On the generation of hot-spots by microwave electric and magnetic fields and their impact on a microwave-assisted heterogeneous reaction in the presence of metallic Pd nanoparticles on an activated carbon support. *J. Phys. Chem. C* **115**, 23030–23035. <https://doi.org/10.1021/jp2076269> (2011).
41. Petricci, E., Risi, C., Ferlin, F., Lanari, D. & Vaccaro, L. Avoiding hot-spots in Microwave-assisted Pd/C catalysed reactions by using the biomass derived solvent γ -Valerolactone. *Sci. Rep.* **8**, 10571. <https://doi.org/10.1038/s41598-018-28458-y> (2018).
42. Horikoshi, S., Osawa, A., Sakamoto, S. & Serpone, N. Control of microwave-generated hot spots. Part V. Mechanisms of hot-spot generation and aggregation of catalyst in a microwave-assisted reaction in toluene catalyzed by Pd-loaded AC particulates. *Appl. Catal. Gen.* **460–461**, 52–60. <https://doi.org/10.1016/j.apcata.2013.04.022> (2013).
43. Radke, W. & Held, D. Tips & tricks GPC/SEC: Polydispersity—How broad is broad for macromolecules?. *Column* **12**, 19–22 (2016).

44. Lemasson, F. *et al.* Polymer library comprising fluorene and carbazole homo- and copolymers for selective single-walled carbon nanotubes extraction. *Macromolecules* **45**, 713–722. <https://doi.org/10.1021/ma201890g> (2012).
45. Chen, F., Wang, B., Chen, Y. & Li, L.-J. Toward the extraction of single species of single-walled carbon nanotubes using fluorene-based polymers. *Nano Lett.* **7**, 3013–3017. <https://doi.org/10.1021/nl071349o> (2007).
46. Schuettfort, T., Snaith, H. J., Nish, A. & Nicholas, R. J. Synthesis and spectroscopic characterization of solution processable highly ordered polythiophene–carbon nanotube nanohybrid structures. *Nanotechnology* **21**, 025201. <https://doi.org/10.1088/0957-4484/21/2/025201> (2010).
47. Gao, J., Kwak, M., Wildeman, J., Herrmann, A. & Loi, M. A. Effectiveness of sorting single-walled carbon nanotubes by diameter using polyfluorene derivatives. *Carbon* **49**, 333–338. <https://doi.org/10.1016/j.carbon.2010.09.036> (2011).
48. Ding, J. *et al.* Enrichment of large-diameter semiconducting SWCNTs by polyfluorene extraction for high network density thin film transistors. *Nanoscale* **6**, 2328. <https://doi.org/10.1039/c3nr05511f> (2014).
49. Cheng, F., Imin, P., Maunders, C., Botton, G. & Adronov, A. Soluble, discrete supramolecular complexes of single-walled carbon nanotubes with fluorene-based conjugated polymers. *Macromolecules* **41**, 2304–2308. <https://doi.org/10.1021/ma702567y> (2008).
50. Berton, N., Lemasson, F., Hennrich, F., Kappes, M. M. & Mayor, M. Influence of molecular weight on selective oligomer-assisted dispersion of single-walled carbon nanotubes and subsequent polymer exchange. *Chem. Commun.* **48**, 2516. <https://doi.org/10.1039/c2cc17508h> (2012).
51. Imin, P., Cheng, F. & Adronov, A. The effect of molecular weight on the supramolecular interaction between a conjugated polymer and single-walled carbon nanotubes. *Polym. Chem.* **2**, 1404. <https://doi.org/10.1039/c1py00023c> (2011).
52. Jakubka, F. *et al.* Effect of polymer molecular weight and solution parameters on selective dispersion of single-walled carbon nanotubes. *ACS Macro Lett.* **1**, 815–819. <https://doi.org/10.1021/mz300147g> (2012).

Acknowledgements

The authors would like to thank the National Science Centre, Poland (under the SONATA program, Grant agreement UMO-2020/39/D/ST5/00285) for supporting the research and the Polish National Agency for Academic Exchange for funding a project within the Strategic Partnerships program (BPI/PST/2021/1/00039) that enabled a visit at the Indian Institute of Technology Roorkee, India to conduct a part of the experimental work.

Author contributions

T.W., D.Ju., A.D., and D.Ja. conceived the study idea. T.W., D.Ju., A.D., D.L., S.W., A.M., S.K., A.B., R.C., and D.Ja. were involved in the data interpretation, and analysis. T.W. and D.Ja. prepared the manuscript. All authors approved the final report.

Competing interests

The authors declare no competing interests.

Additional information

Supplementary Information The online version contains supplementary material available at <https://doi.org/10.1038/s41598-024-52795-w>.

Correspondence and requests for materials should be addressed to D.J.

Reprints and permissions information is available at www.nature.com/reprints.

Publisher's note Springer Nature remains neutral with regard to jurisdictional claims in published maps and institutional affiliations.



Open Access This article is licensed under a Creative Commons Attribution 4.0 International License, which permits use, sharing, adaptation, distribution and reproduction in any medium or format, as long as you give appropriate credit to the original author(s) and the source, provide a link to the Creative Commons licence, and indicate if changes were made. The images or other third party material in this article are included in the article's Creative Commons licence, unless indicated otherwise in a credit line to the material. If material is not included in the article's Creative Commons licence and your intended use is not permitted by statutory regulation or exceeds the permitted use, you will need to obtain permission directly from the copyright holder. To view a copy of this licence, visit <http://creativecommons.org/licenses/by/4.0/>.

© The Author(s) 2024